Resonance fluorescence of an adatom near solid surfaces

Xiao-shen Li and Chang-de Gong
Department of Physics, Nanjing University, Nanjing, Jiangsu, People's Republic of China
(Received 16 June 1986)

By using the reservoir theory and Dekker's quantization procedure for a dissipation system, a set of new surface-dressed optical Bloch equations including the surface-induced frequency shift as well as the decay rate is derived to calculate the resonance fluorescence spectrum of an adatom near a bulk solid surface. A mediate layer composed of nonabsorbing dielectric is placed to separate the adatom and the bulk solid. The size and the dielectric effects of this layer are found to be as important as those effects from the bulk solid. These effects will be directly exhibited in the decay rates and the frequency shifts. The resonance fluorescence spectrum is discussed in different cases and is found to be strongly affected by the surfaces.

I. INTRODUCTION

There has been considerable interest during the past one or two decades in the interaction of atoms or molecules absorbed at solid surfaces with radiation fields.[1-7] The effects of the solid surfaces on the optical properties of the adatoms such as spontaneous emission,[1,3] Raman scattering,[2] and weak- or strong-field resonance fluorescence[4-7] are remarkable. Therefore, the optical properties of absorbed atoms may be used as a sensitive probe of the electronic and other structure of their solid substrates.[8] Here we shall study the process of resonance fluorescence of an atom or molecule at a solid surface.

It is well known that the optical Bloch equations[9] are very useful and thus widely used in dealing with the interaction of light with atoms in gases or solids. Here we shall provide surface-dressed optical Bloch equations (SBE) which are different from those derived by Huang *et al.*[4-7,10] In our calculation of the scattering spectrum for the two-level adatom, the following factors have been considered:

(i) vacuum fluctuations and atomic collision,
(ii) irradiation of external monochromatic field and surface-reflected field,
(iii) size and dielectric effects of a dielectric layer between a bulk solid occupying semi-infinite region and the adatom,
(iv) polariton in the dielectric layer and at the surfaces, and
(v) dissipation in the interaction between the adatom and the surface-reflected field.

Meanwhile, we have also considered the case when the bulk solid is a perfect conductor or a dielectric of which the transverse frequency coincides with that of the adatomic transition.

In Sec. II we use the reservoir method[11,12] and extend Dekker's quantization procedure[13] for a dissipation system to obtain the SBE. In Sec. III we calculate the surface-reflected field by using Maxwell's equations and obtain the decay rates and frequency shifts induced by the surfaces and then make some discussions about them. In Sec. IV we obtain the resonance fluorescence spectrum by means of the SBE and the regression theorem for correlation functions. The effects of the distance between the adatom and the bulk solid (or the thickness of the mediate layer) on the spectrum are discussed in detail. In Sec. V we give some concluding remarks.

II. DERIVATION OF THE SBE

In this paper we consider a two-level atom adsorbed on the surface of a layer of nonabsorbing dielectric which is fixed on the surface of a bulk solid. The geometry of this problem is shown in Fig. 1 in which the thickness of the layer can be changed to determine the various distances d between the atom and the bulk solid.[5] The atom is then excited by the external laser field and thus emits radiation fields which are reflected by the surfaces. The reflected field in turn acts on the atom and influences its dynamic behavior.

To treat this problem we use the reservoir theory[11] shown in Fig. 2 and the self-consistent method.[3,4] In the former the atom is coupled with dissipation reservoirs composed of vacuum fluctuations, collisions with foreign atoms in the gas medium above the layer, and interaction

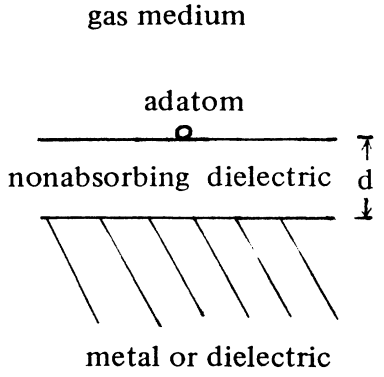

FIG. 1. Geometry for the present problem.

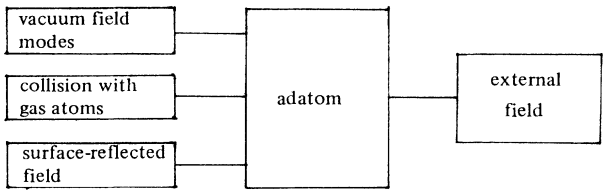

FIG. 2. The adatom coupled with its reservoirs and the external field.

with surface-reflected fields, while in the latter the dipole moment of the adatom is first determined by the SBE in which the reflected field is unknown. Then the dipole moment is used in Maxwell's equations to determine the reflected field which in turn returns to SBE to find the dipole moment.

As in the reservoir theory, the density operator for the adatom obeys the following equation:

$$\dot{\rho}=\dot{\rho}_A+\dot{\rho}_R+\dot{\rho}_{\text{ext}} , \tag{1}$$

where ρ_A, ρ_R, and ρ_{ext} denote the surface-free part, the surface part, and that from the external laser field, respectively. ρ_A and ρ_{ext} can be determined by [in the rotating-wave approximation (RWA)][12]

$$\dot{\rho}_A=-i\omega_{21}[S^z,\rho]-A(S^+S^-\rho-2S^-\rho S^++\rho S^+S^-) \tag{2}$$

and

$$\dot{\rho}_{\text{ext}}=-i[H_{\text{ext}},\rho] , \tag{3}$$

respectively, where ω_{21} is the transition frequency between two levels $|2\rangle$ and $|1\rangle$, A is the Einstein's decay coefficient,

$$S^+=|2\rangle\langle 1| \tag{4}$$

and

$$S^-=|1\rangle\langle 2| , \tag{5}$$

$$S^z=\tfrac{1}{2}(|2\rangle\langle 2|-|1\rangle\langle 1|) \tag{6}$$

are the atomic dipole operators and the inversion operator,[12] respectively, and the Hamiltonian for the interaction between the atom and the external field is

$$H_{\text{ext}}=-|P|(ES^-e^{i\omega_L t}+E^*S^+e^{-i\omega_L t}) , \tag{7}$$

where $|P|$ is the matrix element of electric dipole operator, E and ω_L are the amplitude and frequency of the driving field, respectively.

As for the contribution from surfaces ρ_R, we have considered that there is dissipation when the adatom is coupled with its reflected field and introduced a complex interaction Hamiltonian in RWA:[12]

$$H_R=-\mathbf{p}\cdot\mathbf{E}_R=-|P|S^-E_R^\dagger=-|P|^2f^*(d)S^-S^+ \tag{8}$$

and its adjoint

$$H_R^\dagger=-|P|E_RS^+=-|P|^2f(d)S^-S^+ , \tag{9}$$

where the reflected field can be written within the RWA as

$$E_R=f(d)|P|S^-=pf(d) , \tag{10}$$

$\mathbf{p}$ is dipole moment, and E_R is the component of $\mathbf{E}_R$ along the direction of $\mathbf{p}$. d is the distance between the adatom and the bulk solid and also the thickness of the supporting layer. Then we use Dekker's quantization procedure[13] for a dissipative system and take S^- and S^+ as complex conjugate variables[14,15] of this system. Therefore, the Liouville equation is

$$\dot{\rho}_R=-i[S^+,[S^-,H_R]\rho]+i[\rho[H_R^\dagger,S^+],S^-] . \tag{11}$$

Using (1)—(11), one can easily obtain the SBE

$$\langle\dot{S}^+\rangle=[i(\omega_{21}+\Omega^s)-\Gamma_2]\langle S^+\rangle+i2|P|Ee^{i\omega_L t}\langle S^z\rangle , \tag{12}$$

$$\langle\dot{S}^z\rangle=-2\Gamma_1(\langle S^z\rangle+\tfrac{1}{2}) -i|P|(\langle S^-\rangle Ee^{i\omega_L t}-\langle S^+\rangle E^*e^{-i\omega_L t}) , \tag{13}$$

$$\langle\dot{S}^-\rangle=-[i(\omega_{21}+\Omega^s)+\Gamma_2]\langle S^-\rangle -i2|P|E^*e^{-i\omega_L t}\langle S^z\rangle , \tag{14}$$

where $\Gamma_1=\gamma^{(0)}+\gamma^s$, $\Gamma_2=\gamma^{(0)}+\gamma^s$, $\gamma^{(0)}=\frac{1}{2}A$, and

$$\Omega^s=|P|^2\text{Re}f(d) \tag{15}$$

and

$$\gamma^s=|P|^2\text{Im}f(d) \tag{16}$$

are the frequency shift and decay rate caused by solid surfaces, respectively. On transforming (12)—(14) to the rotating frame, i.e., replacing S^- and S^+ by $S^-e^{-i\omega_L t}$ and $S^+e^{i\omega_L t}$, we obtain the reduced SBE

$$\langle\dot{S}^+\rangle=[i(\Delta+\Omega^s)-\Gamma_2]\langle S^+\rangle+i2\Omega\langle S^z\rangle , \tag{17}$$

$$\langle\dot{S}^z\rangle=-2\Gamma_1(\langle S^z\rangle+\tfrac{1}{2})-i\Omega\langle S^-\rangle+i\Omega^*\langle S^+\rangle , \tag{18}$$

$$\langle\dot{S}^-\rangle=-[i(\Delta+\Omega^s)+\Gamma_2]\langle S^-\rangle-i2\Omega\langle S^z\rangle , \tag{19}$$

where $\Delta=\omega_{21}-\omega_L$, $\Omega=|P|E$ is half the Rabi frequency, and we have taken into account the collision effects and thus Γ_1 and Γ_2 have been rewritten as

$$\Gamma_1=\gamma^{(0)}+\gamma^s+\tfrac{1}{2}\gamma_I , \tag{20}$$

$$\Gamma_2=\gamma^{(0)}+\gamma^s+\tfrac{1}{2}\gamma_I+\tfrac{1}{2}\gamma_E , \tag{21}$$

where γ_I and γ_E are the mean rate of inelastic and elastic collisions,[16] respectively.

Our SBE, Eqs. (17)—(19), are apparently different from those derived by Huang *et al.*[4–7,10] Firstly, here the frequency shift caused by the surfaces is taken into account. However, the method used by Huang *et al.* fails to include the real part of the reflected field leading to the frequency shift. Secondly, from our SBE one can see that the influence of the surfaces appear not only in the decay rates of $\langle S^+\rangle$ and $\langle S^-\rangle$ but also in that of $\langle S^z\rangle$, while in the SBE derived by Huang *et al.*, the presence of the surface only affected $\langle S^+\rangle$ and $\langle S^-\rangle$. In addition, the reflected field E_R is also different, which will be shown later.

III. THE REFLECTED FIELD

In this section we calculate the surface-reflected field. As shown in Fig. 1, the adatom can be taken as an emitting dipole located at the interface between the nonabsorbing dielectric layer and the gas medium. The emitted field is reflected by both the above interface and the one between the layer and the bulk solid. The reflected electric field at the dipole position is what we proceed to find.

First, we consider the general case, i.e., there is an emitting dipole located at $\mathbf{r}=\mathbf{r}_0$ in the region $-\infty \le z \le -d$ which is called region III and filled with gas medium ($\epsilon_3=1$). The nonabsorbing dielectric layer occupies volume $-d \le z \le 0$ called region II and the bulk solid occupies the region $0 \le z \le \infty$ called region I.

From the Maxwell's equations

$$\nabla\times\mathbf{E}=-\frac{1}{c}\frac{\partial}{\partial t}\mathbf{B}\ ,$$
$$\nabla\times\mathbf{B}=0\ ,$$
$$\nabla\times\mathbf{H}=\frac{1}{c}\frac{\partial}{\partial t}(\mathbf{D}+4\pi\mathscr{P})\ ,$$
$$\nabla\cdot(\mathbf{D}+4\pi\mathscr{P})=0\ ,$$

and the expression for the dipole moment

$$\mathscr{P}(\mathbf{r},\omega)=\mathbf{p}(\omega)\delta(\mathbf{r}-\mathbf{r}_0)\ , \tag{22}$$

we obtain the following set of equations:[3]

$$\nabla^2\mathbf{E}_1+k_0^2\epsilon_1\mathbf{E}_1=0,\quad \nabla\cdot\mathbf{E}_1=0$$
$$\mathbf{H}_1=\nabla\times\mathbf{E}_1/ik_0 \tag{23}$$

for region I;

$$\nabla^2\mathbf{E}_2+k_0^2\epsilon_2\mathbf{E}_2=0,\quad \nabla\cdot\mathbf{E}_2=0$$
$$\mathbf{H}_2=\nabla\times\mathbf{E}_2/ik_0 \tag{24}$$

for region II; and

$$\nabla^2\mathbf{E}_3+k_0^2\mathbf{E}_3=-4\pi[k_0^2\mathscr{P}+\nabla(\nabla\cdot\mathscr{P})]\ ,$$
$$\mathbf{H}_3=\nabla\times\mathbf{E}_3/ik_0 \tag{25}$$

for region III, where $k_0=\omega/c$. The solution for the electric field of the above equations can be written as[3]

$$\mathbf{E}_1(\mathbf{r},\omega)=\int\int\mathscr{E}_1(u,v,\omega)e^{i\mathbf{k}_1\cdot\mathbf{r}}du\,dv,\quad \mathbf{k}_1\cdot\mathscr{E}_1=0$$
$$\mathbf{k}_1=(u,v,w_1),\quad w_1^2=k_0^2\epsilon_1-u^2-v^2,\quad \mathrm{Im}w_1\ge 0 \tag{26}$$

$$\mathbf{E}_2(\mathbf{r},\omega)=\int\int[\mathscr{E}_2^{(+)}(u,v,\omega)e^{i\mathbf{k}_2\cdot\mathbf{r}}+\mathscr{E}_2^{(-)}(u,v,\omega)e^{i\mathbf{k}_2'\cdot\mathbf{r}}]du\,dv\ ,$$
$$\mathbf{k}_2\cdot\mathscr{E}_2^{(+)}=0,\quad \mathbf{k}_2'\cdot\mathscr{E}_2^{(-)}=0,\quad \mathbf{k}_2=(u,v,w_2) \tag{27}$$
$$\mathbf{k}_2'=(u,v,-w_2),\quad w_2^2=k_0^2\epsilon_2-u^2-v^2$$

$$\mathbf{E}_3(\mathbf{r},\omega)=\int\int\mathscr{E}_3(u,v,\omega)e^{i\mathbf{k}_0'\cdot\mathbf{r}}du\,dv+\mathbf{E}_p\ ,$$
$$\mathbf{k}_0'\cdot\mathscr{E}_3=0,\quad \mathbf{k}_0'=(u,v,-w_0),\quad w_0^2=k_0^2-u^2-v^2\ , \tag{28}$$
$$\mathrm{Im}w_0\ge 0$$

$$\mathbf{E}_p(\mathbf{r},\omega)=\frac{i}{2\pi}\int\int\frac{du\,dv}{w_0}[k_0^2\mathbf{p}+\nabla(\mathbf{p}\cdot\nabla)]\times\exp[iu(x-x_0)+iv(y-y_0)+iw_0|z-z_0|]\ .$$

Applying Maxwell boundary conditions at $z=0$ and $z=-d$ and using the same procedure as Ref. 3, we obtain

$$\mathbf{k}_{||}\cdot\mathscr{E}_{3||}=\frac{i}{2\pi}e^{-i\mathbf{k}_0\cdot\mathbf{r}_0-i2w_0d}[k_{||}^2p_\perp-w_0(\mathbf{k}_{||}\cdot\mathbf{p}_{||})]D_1^{-1}\left[\frac{\epsilon_1w_2-\epsilon_2w_1}{\epsilon_1w_2+\epsilon_2w_1}e^{i2w_2d}+\frac{\epsilon_2w_0-w_2}{\epsilon_2w_0+w_2}\right]\ , \tag{29}$$

$$\mathbf{k}_{||}\times\mathscr{E}_{3||}=-\frac{i}{2\pi}e^{-i\mathbf{k}_0\cdot\mathbf{r}_0-i2w_0d}k_0^2D_2^{-1}(\mathbf{k}_{||}\times\mathbf{p}_{||})\left[\frac{w_1-w_2}{w_1+w_2}e^{i2w_2d}+\frac{w_2-w_0}{w_2+w_0}\right]\ , \tag{30}$$

where

$$D_1=1+\frac{\epsilon_2w_0-w_2}{\epsilon_2w_0+w_2}\frac{\epsilon_1w_2-\epsilon_2w_1}{\epsilon_1w_2+\epsilon_2w_1}e^{i2w_2d}\ , \tag{31}$$

$$D_2=1+\frac{w_1-w_2}{w_1+w_2}\frac{w_2-w_0}{w_2+w_0}e^{i2w_2d}\ , \tag{32}$$

the subscript $||$ ($\perp$) means parallel (perpendicular) to the surface $z=0$. Using (29)–(32), we obtain the component of reflected electric field along the dipole direction at $\mathbf{r}$ in region III:

$$E_{R||}(\mathbf{r},\omega)=-\frac{i}{4\pi}p\int\int\frac{du\,dv}{w_0}e^{i\mathbf{k}_0'\cdot\mathbf{r}-i\mathbf{k}_0\cdot\mathbf{r}_0-i2w_0d}\left[w_0^2D_1^{-1}\left[\frac{\epsilon_2w_0-w_2}{\epsilon_2w_0+w_2}+\frac{\epsilon_1w_2-\epsilon_2w_1}{\epsilon_1w_2+\epsilon_2w_1}e^{i2w_2d}\right]+k_0^2D_2^{-1}\left[\frac{w_2-w_0}{w_2+w_0}+\frac{w_1-w_2}{w_1+w_2}e^{i2w_2d}\right]\right]\ , \tag{33}$$

for the case of the dipole oriented parallel to the surface;

$$E_{R\perp}(\mathbf{r},\omega)=\frac{i}{2\pi}p\int\int\frac{du\,dv}{w_0}e^{ik_0'\cdot r-ik_0\cdot r_0-i2w_0d}k_{\parallel}^2D_1^{-1}\left[\frac{\epsilon_2w_0-w_2}{\epsilon_2w_0+w_2}+\frac{\epsilon_1w_2-\epsilon_2w_1}{\epsilon_1w_2+\epsilon_2w_1}e^{i2w_2d}\right], \tag{34}$$

for the perpendicular case.

In this paper we are restricted to the case that the bulk solid is a perfect conductor or a dielectric with its transverse frequency[3] coinciding with the resonant frequency of the adatom. So we have the reflected field at the dipole position, i.e., $\mathbf{r}_0=\mathbf{r}=(0,0,-d)$:

$$E_{R\parallel}=-\frac{i}{2}k_0^3p\int_0^\infty\frac{kdk}{\mu}\left[\mu^2\frac{\epsilon_2\mu-\mu_2+(\epsilon_2\mu+\mu_2)\exp(i\mu_2\hat{d})}{\epsilon_2\mu+\mu_2+(\epsilon_2\mu-\mu_2)\exp(i\mu_2\hat{d})}+\frac{\mu_2-\mu+(\mu_2+\mu)\exp(i\mu_2\hat{d})}{\mu_2+\mu+(\mu_2-\mu)\exp(i\mu_2\hat{d})}\right], \tag{35}$$

$$E_{R\perp}=ik_0^3p\int_0^\infty\frac{k^3dk}{\mu}\frac{\epsilon_2\mu-\mu_2+(\epsilon_2\mu+\mu_2)\exp(i\mu_2\hat{d})}{\epsilon_2\mu+\mu_2+(\epsilon_2\mu-\mu_2)\exp(i\mu_2\hat{d})}, \tag{36}$$

where

$$\mu^2=1-k^2,\quad \mu_2^2=\epsilon_2-k^2,\quad k=k_{\parallel}/k_0,\quad \hat{d}=2\omega d/c\ . \tag{37}$$

From (35) and (36), we obtain

$$f_{\parallel}(d)=-\frac{i}{4}k_0^3\int_0^\infty\frac{ds}{\mu}[\mu^2f_1(s)+f_2(s)], \tag{38}$$

$$f_{\perp}(d)=\frac{i}{2}k_0^3\int_0^\infty\frac{sds}{\mu}f_1(s), \tag{39}$$

where we have $s=k^2$ and

$$f_1(s)=\frac{\epsilon_2\mu+i\mu_2\tan(\mu_2\hat{d}/2)}{\epsilon_2\mu-i\mu_2\tan(\mu_2\hat{d}/2)}, \tag{40}$$

$$f_2(s)=\frac{\mu_2+i\mu\tan(\mu_2\hat{d}/2)}{\mu_2-i\mu\tan(\mu_2\hat{d}/2)}. \tag{41}$$

Evidently $f_1(s)$ and $f_2(s)$ contain resonant denominators resulting from the surface polariton.[3] From (29)—(32) one can see that the resonant denominator of f_1 (f_2) results from TM (TE) modes.[3] It is easy to show that all the poles at positions s_i which satisfy

$$\epsilon_2\mu=i\mu_2\tan(\mu_2\hat{d}/2) \tag{42}$$

and

$$\mu_2=i\mu\tan(\mu_2\hat{d}/2) \tag{43}$$

are of first order. Therefore, we can separate $f_1(s)$ and $f_2(s)$ into two parts of which one is analytic and the other contains poles, i.e.,

$$f_1(s)=f_1^{\mathrm{anl}}(s)+\sum_i\frac{\mathrm{Res}f_1(s_i)}{s-(s_i+i0^+)}, \tag{44}$$

$$f_2(s)=f_2^{\mathrm{anl}}(s)+\sum_i\frac{\mathrm{Res}f_2(s_i)}{s-(s_i+i0^+)}, \tag{45}$$

where $\mathrm{Res}f_{1,2}(s_i)$ denote the residue of $f_{1,2}(s)$ at s_i and are found to be

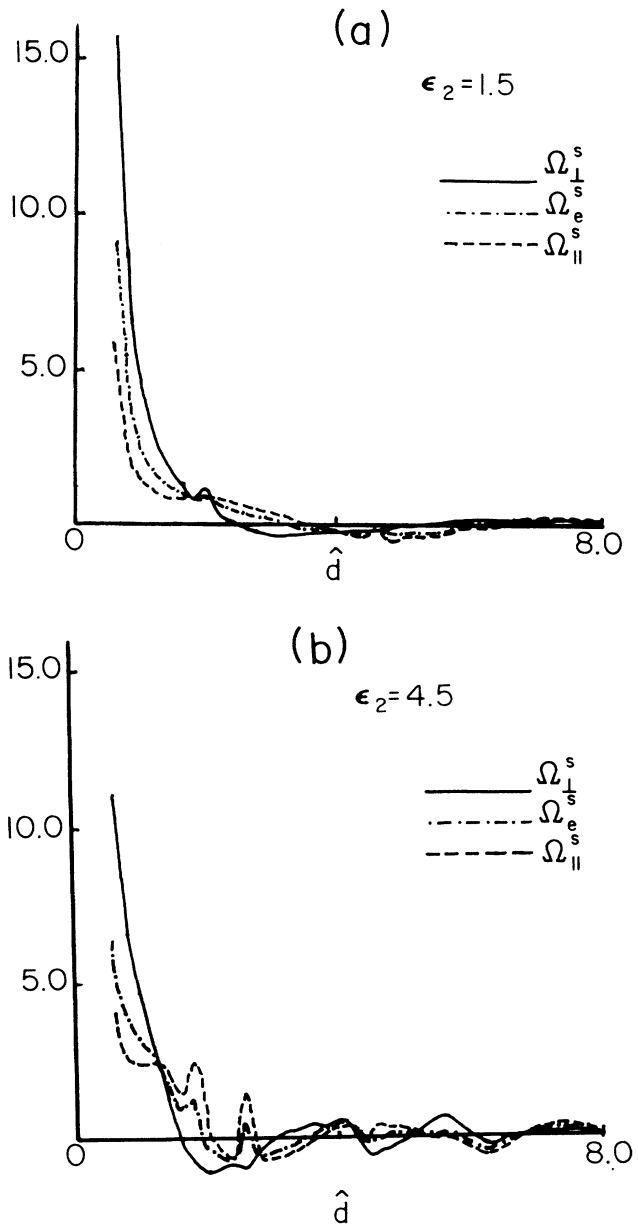

FIG. 3. Frequency shift vs thickness $\hat{d}$ for different orientations of the dipole.

$$\mathrm{Res}f_1(s_i)=4\epsilon_2|\mu|/[\epsilon_2/|\mu|+\epsilon_2|\mu|/\mu_2^2+\tfrac{1}{2}\hat{d}(1+\epsilon_2^2|\mu|^2/\mu_2^2)]|_{s=s_i}\,, \tag{46}$$

$$\mathrm{Res}f_2(s_i)=-4\mu_2/[\mu_2^{-1}+\mu_2/|\mu|^2+\tfrac{1}{2}\hat{d}(|\mu|/\mu_2)(1+\mu_2^2/|\mu|^2)]|_{s=s_i}\,, \tag{47}$$

where we have noticed that solutions of (42) or (43) are in the region $1<s_i<\epsilon_2$ and thus $|\mu|^2=s-1$.

Using (15), (16), (38), (39), and (44)—(47), one can easily find the frequency shifts and decay rates for both the parallel and the perpendicular cases:

$$\Omega_{\parallel}^s=\tfrac{3}{8}\gamma^{(0)}\mathrm{Im}\fint_0^\infty ds[\mu f_1(s)+f_2(s)/\mu]\,, \tag{48}$$

$$\Omega_{\perp}^s=-\tfrac{3}{4}\gamma^{(0)}\mathrm{Im}\fint_0^\infty \frac{sds}{\mu}f_1(s)\,, \tag{49}$$

$$\gamma_{\parallel}^s=-\tfrac{3}{8}\gamma^{(0)}\int_0^1 ds[\mu f_1(s)+f_2(s)/\mu]+\tfrac{3}{8}\pi\gamma^{(0)}\left[\sum_i|\mu|_{s_i}\mathrm{Res}f_1(s_i)-\sum_i\mathrm{Res}f_2(s_i)/|\mu|_{s_i}\right]$$
$$=\Gamma_{\parallel}^b+\Gamma_{\parallel}^p\,, \tag{50}$$

$$\gamma_{\perp}^s=\tfrac{3}{4}\gamma^{(0)}\int_0^1\frac{sds}{\mu}f_1(s)+\tfrac{3}{4}\pi\gamma^{(0)}\sum_i s_i\mathrm{Res}f_1(s_i)|\mu|_{s_i}$$
$$=\Gamma_{\perp}^b+\Gamma_{\perp}^p\,, \tag{51}$$

where $\fint_0^\infty$ denotes the principal value of the integral and $\Gamma_{\parallel}^b$ ($\Gamma_{\perp}^b$) and $\Gamma_{\parallel}^p$ ($\Gamma_{\perp}^p$) the contributions from bulk solid and surface polariton, respectively. However, the contribution of surface polariton to Ω^s cannot be explicitly separated. In this paper, what concerns us is the effects of the bulk solid on the adatom's optical properties. So we subtract from the frequency shift the value for $d\to\infty$ which has nothing to do with the bulk solid and then is included in ω_{21}. Namely, we may replace $\Omega_{\parallel}^s$ and $\Omega_{\perp}^s$ by

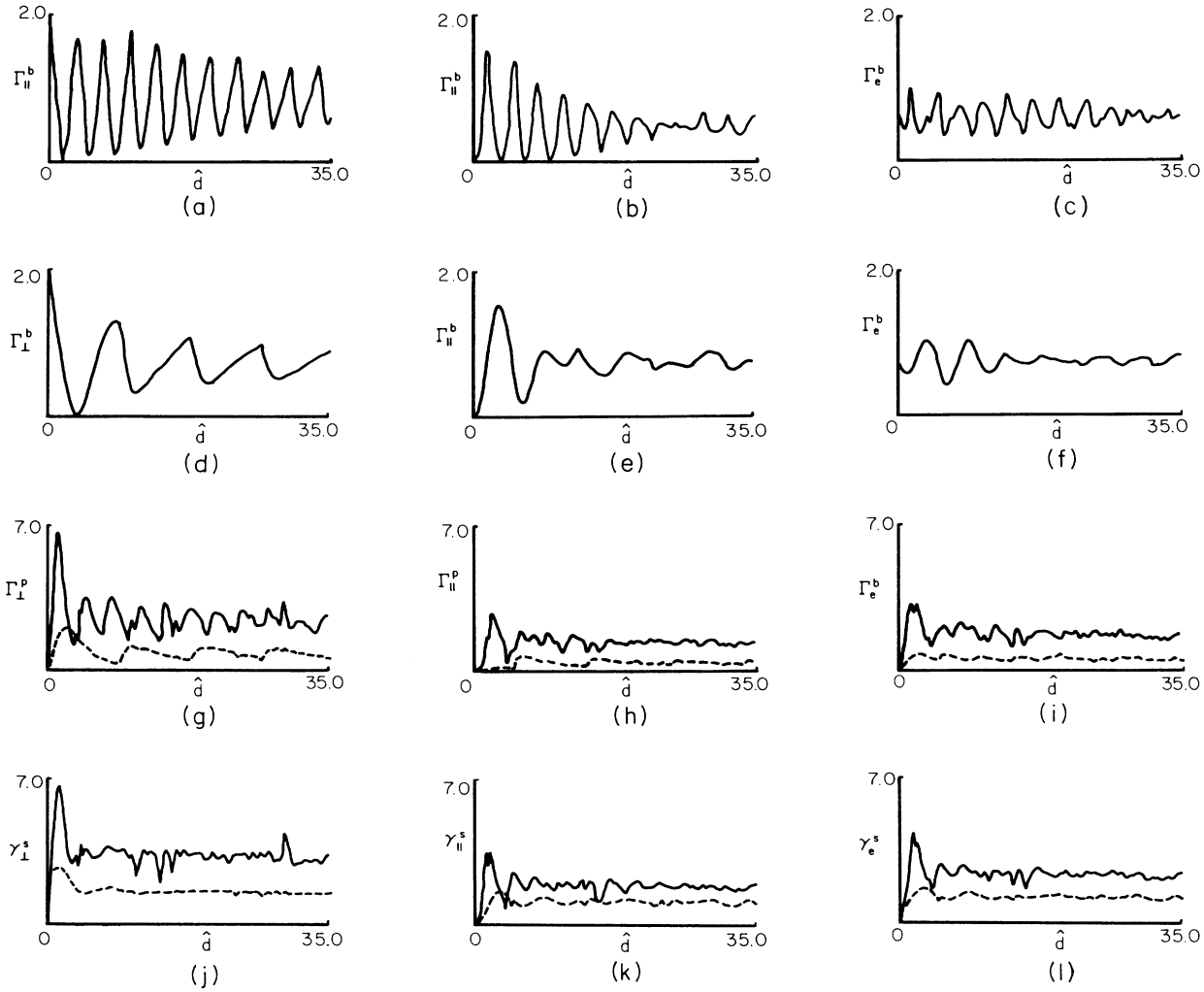

FIG. 4. Decay rates vs thickness $\hat{d}$. (a)—(c) $\epsilon_2=1.5$; (d)—(f) $\epsilon_2=4.5$; (g)—(l) solid curves for $\epsilon_2=4.5$ and dashed curves for $\epsilon_2=1.5$.

$\Omega_{||}^s-\Omega_{||}^s(d\to\infty)$ and $\Omega_{\perp}^s-\Omega_{\perp}^s(d\to\infty)$, respectively. In addition, for an isotropic distribution of dipole orientation usually considered, we have the effective frequency shift

$$\Omega_e^s=\tfrac{2}{3}\Omega_{||}^s+\tfrac{1}{3}\Omega_{\perp}^s \tag{52a}$$

and decay rate

$$\gamma_e^s=\tfrac{2}{3}\gamma_{||}^s+\tfrac{1}{3}\gamma_{\perp}^s\ , \tag{52b}$$

respectively.

Equations (48)—(52) can be calculated numerically and the results are shown in Figs. 3 and 4. From Fig. 3 one can see that the frequency shifts oscillate around zero as $\hat{d}$ increases, die out when $\hat{d}$ becomes very large, and for small $\hat{d}$ Ω^s's become very large. Meanwhile, large ϵ_2 will cause higher frequency of the oscillation but smaller Ω^s's for small $\hat{d}$, and the quantities for different orientations of the dipole are apparently different. This means that the influence of the bulk solid becomes weaker when the adatom is located far from it, stronger when near it, and oscillatory for mediate distance; and that the orientation of the dipole and the dielectric property of the layer play an important role. The following reason is evident: the amplitude and the phase of the reflected field of which the vertical (parallel) component interacts only with the dipole oriented vertically (parallel) are affected not only by the distance $\hat{d}$ but also by the dielectric constant of the layer ϵ_2. This is also true for the decay rates. From Fig. 4 we can see the oscillatory behavior of decay rate in various cases. Generally speaking, the oscillations decay as $\hat{d}$ increases. However, as shown in Figs. 4(b) and 4(e), the oscillations for Γ^b's exhibit revival resulting from the fact that there is coherence between the field reflected by the surface of the bulk solid and that of the dielectric layer. As the adatom is located just on the surface of the layer, the influence of the surface polariton is remarkable. Evidently, the contribution from the surface polariton is greater than that from the bulk solid. In addition, the influence of the dielectric properties of the layer is also very remarkable, i.e., the larger the ϵ_2 is, the higher the frequency of the oscillations and the larger the total decay rates γ^s's will be. We must notice that d is not only the distance between the adatom and the bulk solid but also the size factor of the mediate layer of which the dielectric property is very important and, subsequently, the effects discussed can be called size and dielectric effects.

IV. RESONANCE FLUORESCENCE SPECTRUM

Now we proceed to find the spectrum of resonance fluorescence which is known to be given by the Fourier transformation of the field correlation function $\langle a^{\dagger}(t'+t)a(t')\rangle$ which is proportional to the atomic correlation function $\langle S^+(t'+t)S^-(t')\rangle$.[12,17–19] Since what we are interested in is the steady-state case, we can use the usual procedure[4–7,16–19] to find the spectrum. In steady state we have $\lim_{t'\to\infty}\langle S^+(t'+t)S^-(t')\rangle=\langle S^+(t)S^-\rangle$. By defining the set of correlation functions

$$\begin{aligned}\psi_1&=\langle S^+(t)S^-\rangle\ ,\\ \psi_2&=\langle S^-(t)S^-\rangle\ ,\\ \psi_3&=\langle S^z(t)S^-\rangle\end{aligned} \tag{53}$$

and using the regression theorem,[20] Eqs. (17)—(19) lead to the following set of equations

$$\dot{\psi}_1=[i(\Omega^s+\Delta)-\Gamma_2]\psi_1+i2\Omega\psi_3\ , \tag{54}$$

$$\dot{\psi}_2=-[i(\Omega^s+\Delta)+\Gamma_2]\psi_2-i2\Omega^*\psi_3\ , \tag{55}$$

$$\dot{\psi}_3=i\Omega^*\psi_1-i\Omega\psi_2-2\Gamma_1(\psi_3+\tfrac{1}{2}\langle S^-\rangle)\ , \tag{56}$$

of which the initial conditions are given by

$$\psi_1(0)=\alpha\,|\,\Omega\,|^2/[\Gamma_2^2+(\Delta+\Omega^s)^2+2\alpha\,|\,\Omega\,|^2]\ , \tag{57}$$

$$\psi_2(0)=0\ , \tag{58}$$

$$\psi_3(0)=-\tfrac{1}{2}\Omega^*[i\Gamma_2+(\Omega^s+\Delta)]/[\Gamma_2^2+(\Delta+\Omega^s)^2+2\alpha\,|\,\Omega\,|^2]\ , \tag{59}$$

where $\alpha=\Gamma_2/\Gamma_1$. With expressions (57)—(59), the Eqs. (54)—(56) can be solved by Laplace transformation:

$$\tilde{\psi}_i(Y)=\int_0^{\infty}e^{-Yt}\psi_i(t)dt\quad(i=1,2,3)\ . \tag{60}$$

The solution related to the spectrum is

$$\begin{aligned}\tilde{\psi}_1(Y)=[&\alpha Y^2+(2\Gamma_2+\alpha X+X^*)Y+|\,X\,|^2\\&+2(\alpha\,|\,\Omega\,|^2+\Gamma_1X^*+\Gamma_2X)\\&+2\Gamma_1\,|\,X\,|^2/Y]\psi_1(0)/\alpha F(Y)\ ,\end{aligned} \tag{61}$$

where

$$\begin{aligned}F(Y)=&Y^3+2(\Gamma_1+\Gamma_2)Y^2+(4\Gamma_1\Gamma_2+4\,|\,\Omega\,|^2+|\,X\,|^2)Y\\&+2\Gamma_1(2\alpha\,|\,\Omega\,|^2+|\,X\,|^2)\ ,\end{aligned} \tag{62}$$

$$X=\Gamma_2+i\Delta',\quad \Delta'=\Omega^s+\Delta\ . \tag{63}$$

Through the usual procedure as in Refs. 17—19, the required spectrum is given by

$$\begin{aligned}\tilde{g}(\omega)=&2\pi A_0^{\rm coh}\delta(\omega-\omega_L)+\frac{A_0^{\rm inc}s_0}{(\omega-\omega_L)^2+s_0^2}\\&+\frac{A_+\sigma}{(\omega-\omega_L+\Omega')^2+\sigma^2}+\frac{A_-\sigma}{(\omega-\omega_L-\Omega')^2+\sigma^2}\\&\text{for }\Omega'\gg\Gamma_1,\Gamma_2\ ,\end{aligned} \tag{64}$$

where

$$A_0^{\rm coh}=|\,\Omega\,|^2\,|\,X\,|^2/Y_1^2\ , \tag{65}$$

$$A_0^{\rm inc}=8\,|\,\Omega\,|^4[\alpha^2\,|\,\Omega\,|^2+(\alpha-1)\Delta'^2]/Y_1^2\ , \tag{66}$$

$$A_{\pm}=|\,\Omega\,|^2(\Omega'\pm\Delta')[\tfrac{1}{2}\alpha(\Omega'\pm\Delta')\mp\Delta']/\Omega'^2Y_1\ , \tag{67}$$

$$s_0=2(\Gamma_1\Delta'^2+2\Gamma_2\,|\,\Omega\,|^2)/\Omega'^2\ , \tag{68}$$

$$\sigma=[4\Gamma_1\,|\,\Omega\,|^2+\Gamma_2(2\,|\,\Omega\,|^2+\Delta'^2)]/\Omega'^2\ , \tag{69}$$

$$\Omega'^2=\Delta'^2+4\,|\,\Omega\,|^2,\quad Y_1=2\alpha\,|\,\Omega\,|^2+\Delta'^2\ . \tag{70}$$

For the case of weak incident field ($|\,\Omega\,|\ll\Gamma_1,\Gamma_2$ or Δ') we find[21]

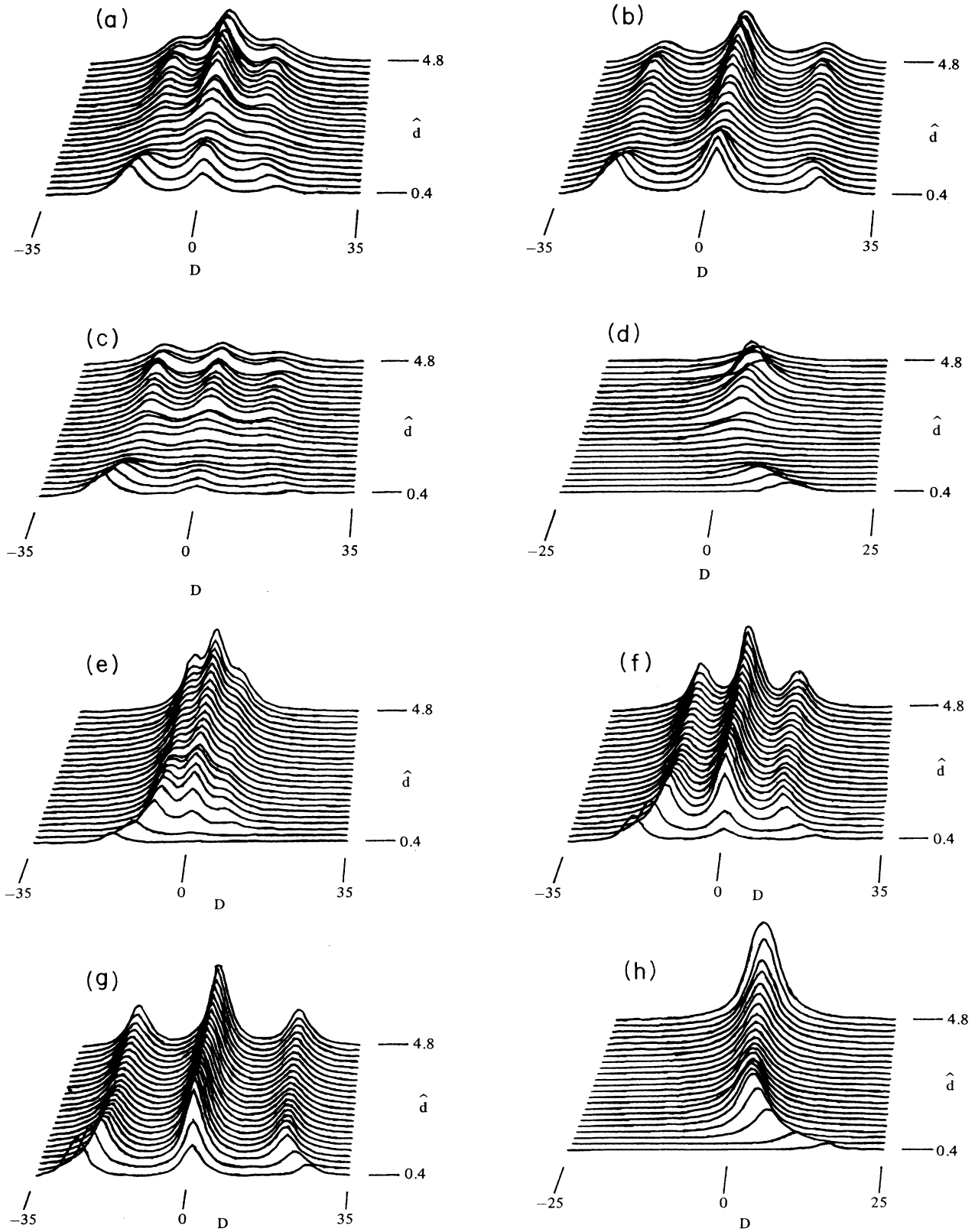

FIG. 5. Resonance fluorescence spectrum vs $D=\omega-\omega_L$ for various choices of thickness $\hat{d}$ when $\gamma_E=1$. (a) $\epsilon_2=4.5$, $|\Omega|=6$, $\Delta=2$; (b) $\epsilon_2=4.5$, $|\Omega|=10$, $\Delta=2$; (c) $\epsilon_2=4.5$, $|\Omega|=6$, $\Delta=8$; (d) $\epsilon_2=4.5$, $|\Omega|=0.2$, $\Delta=2$; (e) $\epsilon_2=1.5$, $|\Omega|=3$, $\Delta=2$; (f) $\epsilon_2=1.5$, $|\Omega|=6$, $\Delta=2$; (g) $\epsilon_2=1.5$, $|\Omega|=10$, $\Delta=2$; (h) $\epsilon_2=1.5$, $|\Omega|=0.2$, $\Delta=2$.

$$\tilde{g}(\omega)=\frac{|\Omega|^2}{|X|^2}\left[2\pi\delta(\omega-\omega_L)+\frac{2(\alpha-1)\Gamma_2}{(\omega-\omega_L-\Delta')^2+\Gamma_2^2}\right]. \tag{71}$$

By considering the isotropic orientation distribution for the dipole and using the unit of $\frac{1}{2}A$ to rescale the $|\Omega|$, Δ, and all the decay rates and frequency shifts, Figs. 5(a)—5(c) and 5(e)—5(g) are numerically obtained from Eq. (64) while Figs. 5(d) and 5(h) are obtained from Eq. (71). Since the coherent component of the spectrum is not shifted or broadened by the surfaces, Figs. 5(a)—5(h) only show the incoherent components. From these figures we can easily see the effects of the surfaces on the resonance fluorescence spectrum of the adatom. When the adatom is located very near the bulk solid, some peaks are suppressed, the existing peaks are broadened and shifted away from the center ($\omega-\omega_L=0$), and for strong excitation, as in Figs. 5(a)—5(c) and 5(e)—5(g), the asymmetry of the two sidebands become remarkable. Comparing Figs. 5(a)—5(d) with Figs. 5(e)—5(h), it is clear that the effects of broadening are stronger for large ϵ_2. This is because the decay rate γ_e^s increases as ϵ_2 increases (see Fig. 4).

As shown in Figs. 5(a)—5(c) and 5(e)—5(g), in the case of strong excitation, there may appear three peaks including the central one resulting from Rayleigh scattering, the left sideband from three-photon process, and the right sideband from fluorescence.[5] From Figs. 5(f) and 5(g) we can see that as $\hat{d}$ increases gradually, the two sidebands will approach to the positions where $D=\pm 2|\Omega|$, respectively. Meanwhile, the three peaks will become narrower and the asymmetry will gradually disappear. The above phenomena appear more or less in the other related figures, where more interesting features are presented. In Fig. 5(e), where ϵ_2 is smaller and the field is weaker than in Figs. 5(f) and 5(g), as $\hat{d}$ increases from 0.4, the profile will change from one sideband to three peaks, then in turn change to two peaks, finally the third peak will gradually emerge. While in Fig. 5(a), where ϵ_2 is large, the profile begins with three peaks, it gradually changes into one central peak, and finally returns to three peaks. The above phenomenon also appears in Fig. 5(b) but less pronouncedly. However, in Fig. 5(c) where detuning Δ is large, all the initial three peaks gradually disappear and then recover.

As for the weak field case shown in Figs. 5(d) and 5(h), there exists only one incoherent peak. In Fig. 5(d) we can see that the peak will shift and disappear then reappear periodically, corresponding to the periodical dependence of γ_e^s and Ω_e^s on $\hat{d}$. However, this interesting phenomenon is not appear clearly in Fig. 5(h). This is because the oscillatory dependence of γ_e^s and Ω_e^s on $\hat{d}$ for smaller ϵ_2 is less pronounced (see Figs. 3 and 4).

In addition, it is evident from Eqs. (64) and (71) that the elastic collision by the gas atoms plays a crucial role in the existence of the asymmetry for the two sidebands and of the incoherent component for weak field.

V. SUMMARY

In this article we have derived a set of new surface-dressed Bloch equations including surface-induced decay rates and frequency shifts, the former are different from those in Refs. 4—7 and the latter are absent in them. By solving the SBE, analytic expressions for resonance fluorescence spectrum of a adatom at solid surface are obtained and the influences of the surfaces on the spectrum are discussed. Under certain circumstances, the existence of the bulk solid and the layer will cause some peaks of the spectrum to disappear or reappear, or to shift and become wider.

[1]R. R. Chance, A. Prock, and R. Silbey, Adv. Chem. Phys. **37**, 1 (1978).

[2]T. E. Furtak and J. Reyes, Surface Sci. **93**, 351 (1980).

[3]G. S. Agarwal, Phys. Rev. A **11**, 230 (1975); **11**, 243 (1975); **11** 253 (1975); **12**, 1475 (1975).

[4]X. Y. Huang, J. T. Lin, and T. F. George, J. Chem. Phys. **80**, 893 (1984).

[5]X. Y. Huang and T. F. George, J. Phys. Chem. **88**, 4801 (1984).

[6]X. Y. Huang, K. C. Liu, and T. F. George, *Laser-Controlled Chemical Processing of Surfaces* (Elsevier, New York, 1984); Mat. Res. Soc. Symp. Proc. **29**, 381 (1984).

[7]X. Y. Huang, T. F. George, and J. Lin, *Coherence and Quantum Optics V* (Plenum, New York, 1984), p. 685.

[8]R. R. Chance, A. Prock, and R. Silbey, Solid State Commun. **18**, 1259 (1976).

[9]L. Allen and J. H. Eberly, *Optical Resonance and Two-Level Atoms* (Wiley, New York, 1975).

[10]J. Lin, X. Y. Huang, and T. F. George, Solid State Commun. **47**, 63 (1983).

[11]M. Sargent, M. O. Scully, and W. E. Lamb, *Laser Physics* (Addison-Wesley, Reading, Mass., 1974).

[12]G. S. Agarwal, *Quantum Statistical Theories of Spontaneous Emission and their Relation to Other Approaches*, Vol. 70 of *Springer Tracts in Modern Physics* (Springer-Verlag, New York, 1974).

[13]H. Dekker, Physica A **95**, 311 (1979).

[14]L. S. Zhang, Physica A **117**, 355 (1983).

[15]F. T. Arecchi, Phys. Rev. A **6**, 2211 (1972).

[16]B. R. Mollow, Phys. Rev. A **15**, 1023 (1977).

[17]B. R. Mollow, Phys. Rev. **188**, 1969 (1969).

[18]H. J. Carmichael and D. F. Walls, J. Phys. B **18**, L685 (1977).

[19]G. S. Agarwal, L. M. Narducci, D. H. Feng, and R. Gilmore, *Coherence and Quantum Optics IV* (Plenum, New York, 1978), p. 281.

[20]M. Lax, Phys. Rev. **157**, 213 (1967).

[21]B. R. Mollow, *Dissipative Systems in Quantum Optics* (Springer-Verlag, New York, 1982), Chap. 2.

[22]R. R. Chance, A. H. Miller, A. Prock, and R. Silbey, J. Chem. Phys. **63**, 1589 (1975).